*The Canadian Mineralogist*
Vol. 40, pp. 1403-1409 (2002)

# DTA, TG, AND XRD STUDIES OF STURMANITE AND ETTRINGITE

SYTLE M. ANTAO

*Center for High Pressure Research (CHiPR) and Department of Geosciences, State University of New York, Stony Brook, N.Y. 11794-2100, U.S.A.*

MICHAEL J. DUANE

*Department of Earth and Environmental Sciences, University of Kuwait, P.O. Box 5969, Safat, 13060, Kuwait*

ISHMAEL HASSAN§

*Department of Chemistry, University of the West Indies, Mona, Kingston 7, Jamaica*

## ABSTRACT

Thermal analyses (DTA and TG) were carried out on sturmanite and ettringite from the Kalahari Manganese Field, South Africa. The TG trace for sturmanite, approximately $Ca_6(Fe^{3+}_{1.5}Al_{0.3}Mn^{2+}_{0.2})_{\Sigma 2.0}\{[B(OH)_4]_{1.2}(SO_4)_{2.3}\}_{\Sigma 3.5}(OH)_{12}\bullet 25H_2O$, indicates that $H_2O(g)$ is lost at about 135°C, $SO_3(g)$ is lost at about 1349°C, and the residue melts at about 1154°C. In sturmanite, a polymorphic transition occurs at about 627°C. For ettringite, approximately $Ca_6Al_2(SO_4)_3(OH)_{12}\bullet 26H_2O$, the $H_2O(g)$ and $SO_3(g)$ are lost at about 149 and 753°C, respectively, and the residue melts at about 1176°C. Ettringite melts after the liberation of both $H_2O(g)$ and $SO_3(g)$, whereas sturmanite melts after the liberation of $H_2O(g)$. The loss of $SO_3(g)$ occurs at a considerably lower temperature in ettringite than in sturmanite. Using powder X-ray diffraction, the unit-cell parameters for sturmanite are *a* 11.157(1), *c* 21.846(3) Å, *V* 2355.2(8) Å$^3$ for the hexagonal supercell, and *a* 11.147(3), *c* 10.918(5) Å, *V* 1174.9(9) Å$^3$ for the subcell. The unit-cell parameters for ettringite are *a* 11.223(1), *c* 21.474(2) Å, *V* 2342.2(5) Å$^3$ for the hexagonal supercell, and *a* 11.229(1), *c* 10.732(2) Å, *V* 1171.9(3) Å$^3$ for the subcell. The volume of sturmanite is only slightly larger than that of ettringite.

*Keywords*: sturmanite, ettringite, differential thermal analysis, thermogravimetric analysis, X-ray diffraction.

## SOMMAIRE

Nous avons effectué des analyses thermiques différentielles et thermogravimétriques de la sturmanite et de l'ettringite provenant du champ minéralisé en manganèse de Kalahari, en Afrique du Sud. Le tracé thermogravimétrique de la sturmanite, dont la composition est proche de $Ca_6(Fe^{3+}_{1.5}Al_{0.3}Mn^{2+}_{0.2})_{\Sigma 2.0}\{[B(OH)_4]_{1.2}(SO_4)_{2.3}\}_{\Sigma 3.5}(OH)_{12}\bullet 25H_2O$, montre qu'il y a perte de $H_2O(g)$ à environ 135°C, et de $SO_3(g)$ à environ 1349°C, et que le résidu passe à l'état fondu à environ 1154°C. La sturmanite subit une transition polymorphique à environ 627°C. Dans le cas de l'ettringite, dont la formule est proche de $Ca_6Al_2(SO_4)_3(OH)_{12}\bullet 26H_2O$, les fractions $H_2O(g)$ et $SO_3(g)$ sont libérées à environ 149 et 753°C, respectivement, et le résidu fond à environ 1176°C. L'ettringite fond après la libération de $H_2O(g)$ et $SO_3(g)$, tandis que la sturmanite fond après la libération de $H_2O(g)$ seul. La fraction $SO_3(g)$ est libérée à une température considérablement plus faible dans le cas de l'ettringite que pour la sturmanite. D'après les données de diffraction X obtenues sur poudre, les paramètres réticulaires de la sturmanite sont *a* 11.157(1), *c* 21.846(3) Å, *V* 2355.2(8) Å$^3$ pour la supermaille hexagonale, et *a* 11.147(3), *c* 10.918(5) Å, *V* 1174.9(9) Å$^3$ pour la sous-maille. Par contre, les paramètres réticulaires de l'ettringite sont *a* 11.223(1), *c* 21.474(2) Å, *V* 2342.2(5) Å$^3$ pour la supermaille hexagonale, et *a* 11.229(1), *c* 10.732(2) Å, *V* 1171.9(3) Å$^3$ pour la sous-maille. Le volume de la sturmanite n'est que faiblement supérieur à celui de l'ettringite.

(Traduit par la Rédaction)

*Mots-clés*: sturmanite, ettringite, analyse thermique différentielle, analyse thermogravimétrique, diffraction X.

§ *E-mail address*: ishmael.hassan@uwimona.edu.jm

## Introduction

Ettringite, approximately $Ca_6Al_2(SO_4)_3(OH)_{12}\bullet 26H_2O$, is an important industrial mineral because of its formation as a product of hydration in Portland and super-sulfated cement, and its use as satin white as a coating material for paper (Moore & Taylor 1970). An exact chemical composition cannot be obtained for ettringite because the $H_2O$ content is variable (McConnell & Murdoch 1962, Moore & Taylor 1970). Sturmanite, approximately $Ca_6(Fe^{3+}_{1.5}Al_{0.3}Mn^{2+}_{0.2})_{\Sigma 2.0}\{[B(OH)_4]_{1.2}(SO_4)_{2.3}\}_{\Sigma 3.5}(OH)_{12}\bullet 25H_2O$, is a ferric iron, boron-containing analogue of ettringite; an exact formula for sturmanite is tentative because of the ambiguity in the number of S and B atoms (Peacor *et al.* 1983). Other minerals in the ettringite group are bentorite [$Ca_6Cr_2(SO_4)_3(OH)_{12}\bullet 26H_2O$, *a* 11.210(15), *c* 21.48(3) Å, space group $P31c$, and $Z = 2$: Gross 1980], jouravskite [$Ca_6Mn_2\{(CO_3)_2(SO_4)_2\}_{\Sigma 4}(OH)_{12}\bullet 24H_2O$, *a* 11.06, *c* 10.50 Å, space group $P6_3/m$, and $Z = 1$: Gaudefroy & Permingeat 1965], and charlesite [$Ca_6(Al,Si)_2\{(B(OH)_4)(SO_4)_2\}_{\Sigma 3}(OH)_{12}\bullet 26H_2O$, *a* 11.16(1), *c* 21.21(2) Å, space group $P31c$, and $Z = 2$: Dunn *et al.* 1983].

Thermal studies have been done on ettringite, but not on sturmanite (*e.g.*, Hall *et al.* 1996, Zhou & Glasser 2001, Wieczorek-Ciurowa *et al.* 2001, Shimada & Young 2001). However, most of these studies pertain to synthetic ettringite and were done in the low-temperature region, <200°C. The chemical compositions of sturmanite and ettringite indicate that $H_2O$ and $SO_3$ are important volatile constituents that may be liberated on heating. This study was carried out to determine what chemical constituents are liberated on heating, to measure the temperature where changes take place, and to compare the results for ettringite and sturmanite, using differential thermal analyses (DTA) and thermogravimetric (TG) analyses to about 1450°C. Unit-cell parameters at room temperature, before heating, were also determined using powder X-ray diffraction (XRD).

## Background Information

The unit cell of ettringite is *a* 11.26, *c* 21.48 Å, $Z = 2$ for the supercell (Bannister *et al.* 1936). The space group for ettringite is $P31c$, and any apparent hexagonal symmetry was attributed to twinning or disorder (Moore & Taylor 1968, 1970, Courtois *et al.* 1968). Peacor *et al.* (1983) suggested that the space group for sturmanite is $P31c$, with unit-cell parameters *a* 11.16(3), *c* 21.79(9) Å for the supercell. They also suggested that the diffraction data for sturmanite are similar to those for the ettringite-group minerals in that sturmanite has a pronounced subcell having parameters $A = a$ and $C = c/2$, *i.e.*, all reflections having $l = 2n + 1$ are very weak, and extinctions are present for reflections $hhl$, $l = 2n + 1$, which is consistent with a glide plane. Ettringite also has a similarly strong subcell to supercell relationship.

The crystal structure of ettringite was studied by several investigators (*e.g.*, Bannister *et al.* 1936, Courtois *et al.* 1968, Moore & Taylor 1968, 1970). Taylor (1973) reviewed the crystal chemistry of the ettringite-group minerals. The ettringite structure consists of columns and channels that are parallel to the *c* axis (Fig. 1; Taylor 1973). The columns contain $[Ca_6[Al(OH)_{12}]\bullet 24H_2O]^{6+}$, and the channels contain $[(SO_4)_3\bullet 2H_2O]^{6-}$, per half unit cell. Each of the columns contains a chain of polyhedra, including one of Al and three of Ca. The $[Al(OH)_6]^{3-}$ octahedra are linked together through three $Ca^{2+}$ ions, which are eightfold co-ordinated by four hydroxyl groups and four $H_2O$ molecules. The $[Al(OH)_6]^{3-}$ octahedron is further co-ordinated by $H_2O$ molecules. The $Ca^{2+}$ polyhedra are trigonal prisms with the axis parallel to ***c***. The $Ca^{2+}$ ion is eightfold coordinated by four $H_2O$ molecules (labeled A and B, Fig. 1) and four OH groups. The A $H_2O$ molecule has nearly the same *Z* coordinate as the $Ca^{2+}$ ion. Each of these prisms shares two edges with adjacent $[Al(OH)_6]^{3-}$ octahedra. Channels between the columns are occupied by $H_2O$ molecules and $SO_4^{2-}$, $CO_3^{2-}$, or $B(OH)_4$ groups. For example, the $SO_4^{2-}$ ions occur on axes along the lines (⅓, ⅔, *z*) and (⅔, ⅓, *z*), in four positions. Statistically, three of these sites are occupied by three $SO_4^{2-}$ groups, and the fourth site by two $H_2O$ molecules. A maximum of four anion groups can occupy these sites, with a corresponding reduction of the two $H_2O$ molecules to zero. If the total number of anion groups is at the maximum number of four, then the number of $H_2O$ molecules is reduced from 26 to 24 in the formula unit. The repeat distance along a column is $C = c/2 = 10.7$ Å, the prominent translation of the substructure, with the superstructure arising from ordering of anionic groups in the sites between the columns. The $Ca^{2+}$ ions may be replaced by ions such as $Pb^{2+}$, and the $Al^{3+}$ by $Fe^{3+}$, $Mn^{3+}$, $Cr^{3+}$, *etc.* (Peacor *et al.* 1983, Wieczorek-Ciurowa *et al.* 2001).

Several thermal studies are available for synthetic ettringite, including some recent investigations (*e.g.*, Hall *et al.* 1996, Zhou & Glasser 2001, Wieczorek-Ciurowa *et al.* 2001, Shimada & Young 2001). In a study of a synthetic ettringite using TG, XRD, and $^{27}Al$ NMR, Shimada & Young (2001) heated ettringite at various temperatures up to 200°C for a period of up to 7 h. The structure maintains some long-range order until the coordination number of Ca changes to 5 by dehydration of 12 $H_2O$ molecules from the channels and columns with heat treatment at 70°C. After 7 hours at 70°C, the short-range order is disrupted, and ettringite becomes XRD-amorphous. Thereafter, the rest of the $H_2O$ molecules in the columns and bridging OH groups in the Ca polyhedra are removed, and the framework of the columns is destroyed. This step is accompanied by changes in the coordination number of Al from 6 to 4 (Shimada & Young 2001).

## Experimental

The samples used in this study are from the Kalahari Manganese Field, South Africa; ettringite is from the N'chwaning II mine, and sturmanite is from the Wessels mine. The samples were coarsely crushed, and pure crystals were handpicked under a binocular microscope. The pure crystals were then crushed to a powder using an agate mortar and pestle. Portions of the powder were used for DTA, TG, XRD, and electron-microprobe analyses.

A weighed amount of powdered sample was placed into an $Al_2O_3$ crucible for thermal analyses. For sturmanite, a fully computerized, Netzsch STA 409 EP/3/D Simultaneous TG–DTA equipment was used. For ettringite, a Shimadzu Thermal System 50 (TG 50 and DTA 50) was used because the first equipment was in need of repairs. Sturmanite was heated at a constant rate of 5°C/min in a static air environment. Ettringite was heated at a rate of 10°C/min. in a dynamic air environment where the flow rate of air was 60 mL/min. Thermal data were analyzed using software programs supplied with the instruments. A detailed experimental procedure is given in Hassan (1996).

XRD data were obtained using a fully computerized Siemens D5000 Diffractometer. The XRD data were obtained with the diffractometer operating in the vertical position and in the θ–θ operating mode. We used Ni-filtered Cu$K\alpha$ radiation in conjunction with a position-sensitive detector. Data were collected at room temperature for the 2θ range of 6 to 110°. A continuous scan was used with a step size of 0.015° and step time of 20.0 s. The unit-cell parameters were obtained by least-squares refinement using the program WIN-METRIC. The zero-shift of the diffractometer was determined by maximizing $F_N$ (a figure-of-merit for all reflections) in the refinement procedure (de Wolff 1968).

The sturmanite sample was used up for thermal analyses. However, for ettringite, we used the available sample for chemical analysis using the electron microprobe (EMP), and for additional XRD runs after heating the sample to 260°C, and then quenching the sample to room temperature. At 260°C, the thermal analyses indicated that all the $H_2O$ molecules were liberated.

The chemical analysis for ettringite was done using a Cameca Camebax electron microprobe using the operating program MBX (copyright by Carl Henderson, University of Michigan) and the correction was done using Cameca's PAP program. The analytical conditions were 15 kV and 9.2 nA beam current. Natural minerals were used as standards: microcline (Si$K\alpha$, K$K\alpha$), albite (Na$K\alpha$), forsterite (Mg$K\alpha$), "apatite" (P$K\alpha$), anorthite (Al$K\alpha$, Ca$K\alpha$), and gypsum (S$K\alpha$). The oxide weight

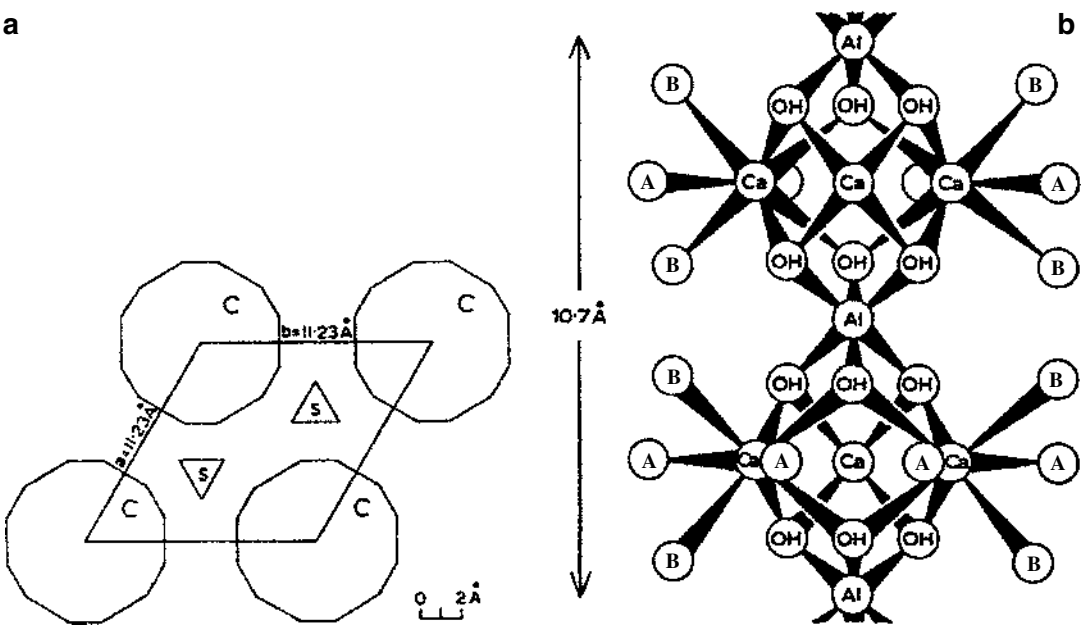


FIG. 1. The general features of the structure of ettringite. (a) Projection along [001] showing the polygons C that represents the columns of $[Ca_3Al(OH)_6{\bullet}12H_2O]^{3+}$, and the triangles S that represents the $SO_4^{2-}$ ions and $H_2O$ molecules in the channels. (b) Part of a column projected on (110). The A and B circles represent $H_2O$ molecules, but those attached to the Ca ions lying in the central vertical line of the figure are omitted, as are all the H atoms (from Taylor 1973).

percentages resulting from the EMP analyses are given in Table 1. The $H_2O$ content for ettringite was obtained by subtraction. Ettringite damages quite easily in the EMP with loss of $SO_3$ and $H_2O$, so a diffuse electron beam was used for the analysis. The results obtained for ettringite are comparable to those in the literature (Table 1).

## Results and Discussion

### *DTA and TG*

Using about 76 mg powder, the TG and DTA curves, and their corresponding derivative curves (DTG and DDTA, respectively) were obtained for sturmanite (Fig. 2). The DTG and DDTA curves were obtained from the corresponding raw data using a narrow window for filtering the measured raw data. The differentiation was done by using a modified Golay–Savitzky algorithm of second order. The characteristic data for sturmanite obtained from these curves are summarized (Table 2). Four peaks are observed in the DTA curve; peaks 1, 2, and 3 are well defined in both the DTA and DDTA curves, but peak 4, although visually detectable, is less obvious, but is clearly seen in the TG and DTG traces (Fig. 2). Peaks 2 and 3 occur as discontinuities only in the DTA trace where there is no loss in weight, so they are attributed to polymorphic phase-transitions. Peak 3 is related to melting of the sturmanite residue because it occurs at a higher temperature compared to peak 2, which is related to a polymorphic transition. A brownish black "melt" was observed in the crucible after the experiment.

There are two well-defined DTG peaks 1 and 4 (Fig. 2a). The sharp peak 1 corresponds to a net loss in weight of 41.6% (Table 2). This weight loss is attributed to the loss of $H_2O$(g). According to the chemical data on sturmanite, $H_2O$ constitutes 46.7 wt.% (Table 1), which is more than the weight loss for peak 1. Peak 4 corresponds to a weight loss of about 12.3%, which is comparable to the 14.2 wt.% of $SO_3$ shown by the chemical analyses (Table 1). Peak 4 is thus attributed to the loss of $SO_3$(g). The loss of weight is more gradual for peak 4 than for peak 1.

Mn is held to be in the 2+ oxidation state in sturmanite (Peacor *et al.* 1983). No oxidation of $Mn^{2+}$ was detected in the DTA and TG analyses of sturmanite, as there was no weight gain. $Mn^{2+}$ should have oxidized to $Mn^{3+}$ starting at about 700°C, as was observed in the DTA and TG analyses of helvite and danalite (Antao & Hassan 2002). The amount of $Mn^{2+}$ present may be too small to be detected by the DTA–TG technique. As an alternative, the Mn may be already trivalent, thus was not oxidized further. Moreover, the presence of $Fe^{3+}$and $Al^{3+}$ suggests that Mn may be present as $Mn^{3+}$ (Peacor *et al.* 1983); however, they tentatively assigned the Mn to $Mn^{2+}$. In helvite and danalite, the oxidized $Mn^{3+}$ cation undergoes further oxidation to $Mn^{4+}$ from about 1300°C (Antao & Hassan 2002), which was also not observed for sturmanite. Jouravskite, an isostructural phase, contains $Mn^{4+}$, and sturmanite could contain Mn in the tetravalent state as well (Peacor *et al.* 1983). In

TABLE 1. CHEMICAL COMPOSITION OF STURMANITE AND ETTRINGITE

| | Sturmanite† | Ideal | Ettringite‡ | Ideal | EMP |
|---|---|---|---|---|---|
| CaO wt % | 25.62 | 25.48 | 26.6 | 26.81 | 26.70 |
| $Na_2O$ | | | | | 0.01 |
| $Fe_2O_3$ | 9.11 | 12.09 | | | |
| MnO | 1.16 | | | | |
| $P_2O_5$ | | | | | 0.20 |
| $Al_2O_3$ | 1.08 | | 7.0 | 8.12 | 9.04 |
| $SiO_2$ | | | | | 0.72 |
| $SO_3$ | 14.02 | 12.13 | 18.8 | 19.14 | 18.67 |
| $B_2O_5$ | 3.18 | 5.27 | | | |
| $H_2O$ | 45.83 | 45.02 | 46.3 | 45.93 | 44.66* |
| others | | | 0.8 | | |
| Total | 100.00 | 100 | 99.5 | 100 | 100 |

† Composition reported by Peacor *et al.* (1983), which leads to the formula $Ca_6(Fe^{3+}_{1.5}Al_{0.5}Mn^{2+}_{0.2})_{\Sigma 2.0}\{[B(OH)_4]_1[SO_4]_{2.1}\}_{\Sigma 3.1}(OH)_{12}{\cdot}25H_2O$.
‡ Composition reported by McConnell & Murdoch (1962).
* $H_2O$ obtained by subtraction. EMP: electron-microprobe data

TABLE 2. DATA FROM THE THERMAL ANALYSIS OF STURMANITE AND ETTRINGITE

| | Sturmanite | | | | Ettringite | | | | |
|---|---|---|---|---|---|---|---|---|---|
| | TG | DTG | DTA | DDTA | TG | DTG | DTA | DDTA | Changes |
| **Peak 1‡** | | | | | | | | | |
| Onset-T (°C) | 102 | 89 | 92 | 125 | 68 | 64 | 93 | 128 | |
| Peak-T (°C) | --- | 135 | 139 | | ---- | 149 | 145 | | Loss of |
| End-T (°C) | 167 | 157 | 181 | 151 | 249 | 201 | 196 | 169 | $H_2O$ |
| % Wt. Loss | 41.6 | | | | 40.4 | | | | (and OH) |
| Enthalpy (J/g) | | | 1660 | | | | 641 | | |
| **Peak 2‡** | | | | | | | | | |
| Onset-T (°C) | | | ---- | | | | | | Poly- |
| Peak-T(°C) | | | -627 | | | | | | morphic |
| End-T (°C) | | | 635 | | | | | | transition |
| **Peak 3‡** | | | | | | | | | |
| Onset-T (°C) | | | 1128 | | | | 1122 | 1164 | Melting |
| Peak-T(°C) | | | 1154 | | | | 1176 | | of |
| End-T (°C) | | | 1156 | | | | 1209 | 1188 | residue |
| **Peak 4§** | | | | | | | | | |
| Onset-T (°C) | 1274 | 1266 | | | 658 | 699 | 708 | | |
| Peak-T(°C) | --- | 1349 | | | --- | 753 | | 732 | Loss of |
| End-T (°C) | 1422 | 1393 | | | 968 | 848 | 765 | | $SO_3$(g) |
| % Wt. Loss | 12.3 | | | | 15.4 | | | | |

‡ exothermic peaks (peaks 1, 2, and 3); § peak 4 is exothermic for sturmanite but endothermic for ettringite. Total % wt. loss for peaks 1 and 4 = –53.9 in sturmanite and –55.8 in ettringite. Total wt. loss from start to finish is –56.9% in sturmanite and –59.7% in ettringite.

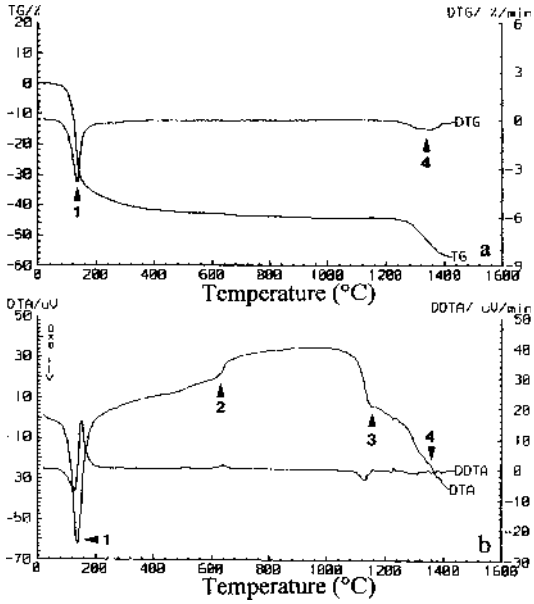


FIG. 2. Sturmanite: (a) TG and DTG curves, and (b) DTA and DDTA curves. Corresponding peaks at a particular temperature are assigned the same number and are labeled on the DTA and DTG curves in this figure and Figure 3.

addition, Cr-substituted ettringite has been synthesized by Wieczorek-Ciurowa *et al.* (2001). Therefore, the present results are most consistent with the hypothesis that the Mn is trivalent.

Thermal curves were obtained for ettringite by using about 10 mg of powder (Fig. 3). Characteristic data for ettringite obtained from these curves are given in Table 2. Three peaks are observed in the DTA trace (peaks 1, 3, and 4; Fig. 3b) and are labeled to correspond to those in sturmanite. Peaks 1 and 3 are well defined in both the DTA and DDTA curves, but peak 4 is clearly seen in the TG and DTG traces (Fig. 3). Peak 3 occurs in the DTA trace, and at that temperature, there is no loss in weight, so peak 3 is attributed to the melting of the residue of ettringite.

Peaks 1 and 4 are well defined in the DTG curve for ettringite (Fig. 3a). As in sturmanite, peaks 1 and 4 correspond to the loss of $H_2O(g)$ and $SO_3(g)$, respectively. The TG curve gives a loss of 40.4% over peak 1 and 15.4% over peak 4 (Table 2). According to the chemical composition of ettringite, $H_2O$ constitutes about 44.7% and $SO_3$ constitutes 18.7% (Table 1). The weight losses obtained from the TG curve are less than those expected from the chemical composition. The rate of loss is slower over peak 4 than over peak 1 (Fig. 3a).

In both ettringite and sturmanite, the observed TG weight loss for $H_2O(g)$ and $SO_3(g)$ are less than those expected from the chemical compositions of the two minerals. With regards to $H_2O$, these differences reflect incomplete liberation of $H_2O$, as was observed for synthetic ettringite by Shimada & Young (2001). They showed that when synthetic ettringite is heated to 120°C, the number of $H_2O$ molecules remaining in the chemical formula is 6.6 with respect to 30.9 $H_2O$ molecules at room temperature. The ideal formula of ettringite is $3CaO{\bullet}Al_2O_3{\bullet}3CaSO_4{\bullet}32H_2O$, which leads to 45.93 wt.% $H_2O$ (Table 1). The TG-established loss of $H_2O$ from ettringite was 41.40 wt.% (Table 2), which corresponds to 26.61 molecules of $H_2O$, so 5.39 molecules of $H_2O$ remained in the sample. These results indicate that natural and synthetic ettringite do behave a little differently. A similar analysis for sturmanite, using the ideal empirical formula, $4CaO{\bullet}Fe_2O_3{\bullet}\frac{1}{2}B_2O_3{\bullet}2CaSO_4{\bullet}33H_2O$, and the TG-established wt.% loss of $H_2O$ (Tables 1, 2), indicates that 4.3 molecules of $H_2O$ remained in the sample.

A batch of ettringite powder was selected for XRD quenching experiments. An XRD trace of the sample, taken at room temperature, indicated that the sample contains a small amount of calcite as an impurity phase (Fig. 4a). This sample was then heated in an oven from room temperature to 260°C at a rate of 5°C/min. At 260°C, the thermal analyses indicated that ettringite is dehydrated. The sample was held at 260°C for one hour and then cooled to room temperature. An XRD trace of

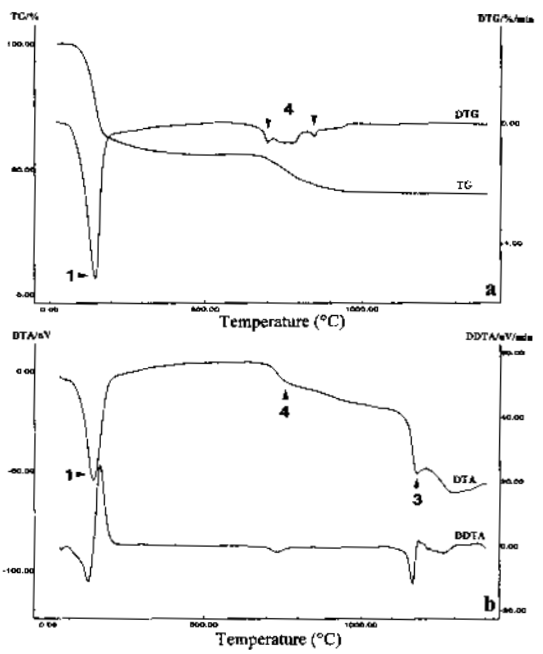


FIG. 3. Ettringite: (a) TG and DTG curves, and (b) DTA and DDTA curves.

the sample contained peaks from ettringite and the impurity calcite phase (Fig. 4b). The same batch was again heated from room temperature to 260°C at a rate of 5°C/min, and the sample was held at 260°C for 7 h and then cooled to room temperature. The XRD trace still showed peaks that are indicative of ettringite and the minor calcite phase (Fig. 4c). These results are in contrast to those obtained for synthetic ettringite by Shimada & Young (2001). When synthetic ettringite is heated to 70°C and held for 7 h, they showed that synthetic ettringite becomes XRD-amorphous, and their XRD trace contained a minor amount of calcite. These conflicting results indicate that synthetic and natural ettringite do behave differently.

In general, both ettringite and sturmanite samples undergo two main well-separated weight-loss stages. The loss of $H_2O$(g) begins at about 68°C in ettringite and at about 102°C in sturmanite. The majority of $H_2O$ molecules escape in a single step, but a significant amount of $H_2O$ remained in the sample. The loss of $SO_3$(g) in ettringite begins at about 658°C, but in sturmanite this loss occurs at a considerably higher temperature, about 1274°C. The $SO_3$(g) escapes in a single step in both samples. In lazurite, the loss of $SO_3$(g) begins at about 1264°C and continues beyond about 1420°C in several steps (Hassan 2000). The temperature at which $SO_3$(g) is liberated in lazurite is comparable to that in sturmanite. The ettringite sample melts after the liberation of both $H_2O$(g) and $SO_3$(g), whereas the sturmanite sample melts after the liberation of $H_2O$(g). The residue of ettringite melts at 1176°C. For sturmanite, the residue melts at 1154°C. The two weight-loss stages begin earlier in ettringite than in sturmanite. These results indicate that the bonds are weaker in ettringite than in sturmanite, which facilitates the escape of volatiles at lower temperatures in ettringite.

*XRD data*

The hexagonal unit-cell obtained in this study for sturmanite is *a* 11.157(1), *c* 21.846(3) Å, *V* 2355.2(8) Å$^3$, with a tolerance in $|2\theta| \leq 0.018°$ for 31 XRD peaks refined in the space group *P*31*c*. The XRD results are similar to those of Peacor *et al.* (1983): *a* 11.16(3), *c* 21.79(9) Å); however, not all their X-ray-diffraction peaks were indexed. All our XRD peaks are indexed, and in particular, a strong 223 peak was observed on the shoulder of the 216 peak; this 223 peak was not observed in the earlier study. The principal X-ray-diffraction peaks are slightly different from those obtained by Peacor *et al.* (1983); in this study they are: [$d_{obs}$ in Å(I)(*hkl*)]: 9.661(100)(100), 5.6 (79)(110), 2.774(72)(304), 2.579(52)(216), and 3.904(48)(114).

Peacor *et al.* (1983) noted that sturmanite has a very pronounced subcell with parameters $A = a$ and $C = c/2$. We have refined the subcell parameters in the space group *P*31*c* and obtained *a* 11.147(3), *c* 10.918(5) Å, *V* 1174.9(9) Å$^3$, with refinement statistics better than those for the supercell.

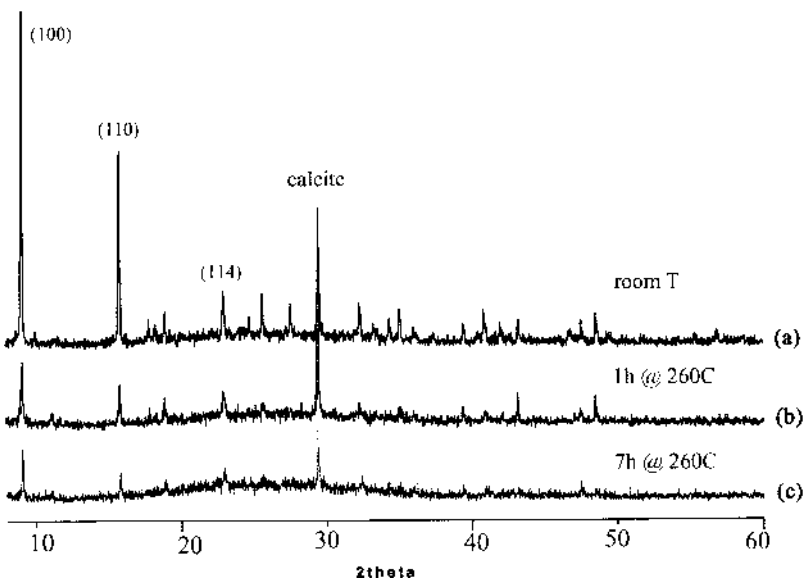


FIG. 4. Ettringite XRD traces: (a) room temperature, (b) heated to 260°C for 1 h, and (c) heated to 260°C for 7 h. The Miller indices of three of the ettringite peaks are labeled. The main peak of calcite is indicated.

The parameters of the hexagonal subcell of ettringite obtained in this study are *a* 11.229(1), *c* 10.732(2) Å, *V* 1171.9(3) Å$^3$, with a tolerance in $|2\theta| \leq 0.025°$ for 48 XRD peaks refined in space group *P*31*c*. The supercell parameters are *a* 11.223(1), *c* 21.474(2) Å, *V* 2342.2(5) Å$^3$, refined in space group $P6_3/mmc$. Comparable values in the literature are *a* 11.26, *c* 21.48 Å (*e.g.*, Bannister *et al.* 1936, Moore & Taylor 1970). The unit-cell volume of sturmanite is slightly larger than that of ettringite. However, volatiles escape from ettringite more easily than from sturmanite.

## Acknowledgements

We thank Nic Beukes and Pieter De Bruyn for providing the ettringite and sturmanite samples, respectively, and D.H. Lindsley for his help with the electron-microprobe analysis, which was financially supported by a NSF grant to J.B. Parise, EAR–0125094. We thank the two anonymous reviewers, Associate Editor M.E. Gunter, and R.F. Martin for useful comments.

## References

Antao, S.M. & Hassan, I. (2002): Thermal analyses of sodalite, tugtupite, danalite, and helvite. *Can. Mineral.* **40**, 163-172.

Bannister, F.A., Hey, M.H. & Bernal, J.D. (1936): Ettringite from Scawt Hill, Co. Antrim. *Mineral. Mag.* **24**, 324-329.

Courtois, A., Dusausoy, Y., Laffaille, A. & Protas, J. (1968): Etude préliminaire de la structure cristalline de l'ettringite. *C.R. Acad. Sci. Paris, Sér.* **D**, **266**, 1911-1913.

de Wolff, P.M. (1968): A simplified criterion for the reliability of a powder pattern indexing. *J. Appl. Crystallogr.* **1**, 108-113.

Dunn, P.J., Peacor, D.R., Leavens, P.B. & Baum, J.L. (1983): Charlesite, a new mineral of the ettringite group, from Franklin, New Jersey. *Am. Mineral.* **68**, 1033-1037.

Gaudefroy, C. & Permingeat, F. (1965): La jouravskite, une nouvelle espèce minérale. *Bull. Soc. Fr. Minéral. Cristallogr.* **88**, 254-262.

Gross, S. (1980): Bentorite, a new mineral from the Hatrurim area, west of the Dead Sea, Israel. *Israel J. Earth Sci.* **29**, 81-84.

Hall, C., Barnes, P., Billimore, A.D., Jupe, A.C. & Turrillas, X. (1996): Thermal decomposition of ettringite $Ca_6[Al(OH)_6]_2(SO_4)_3 \cdot 26H_2O$. *J. Chem. Soc., Faraday Trans.* **92**, 2125-2129.

Hassan, I. (1996): The thermal behavior of cancrinite. *Can. Mineral.* **34**, 893-900.

_____ (2000): Transmission electron microscopy and differential thermal studies of lazurite polymorphs. *Am. Mineral.* **85**, 1383-1389.

McConnell, D. & Murdoch, J. (1962): Crystal chemistry of ettringite. *Mineral. Mag.* **33**, 59-64.

Moore, A.E. & Taylor, H.F.W. (1968): Crystal structure of ettringite. *Nature* **218**, 1048-1049.

_____ & _____ (1970): Crystal structure of ettringite. *Acta Crystallogr.* **B26**, 386-393.

Peacor, D.R., Dunn, P.J. & Duggan, M. (1983): Sturmanite, a ferric iron, boron analogue of ettringite. *Can. Mineral.* **21**, 705-709.

Shimada, Y. & Young, J.F. (2001): Structural changes during thermal dehydration of ettringite. *Advances in Cement Research* **13**, 77-81.

Taylor, H.F.W. (1973): Crystal structures of some double hydroxide minerals. *Mineral Mag.* **39**, 377-389.

Wieczorek-Ciurowa, K., Fela, K. & Kozak, A.J. (2001): Chromium(iii)-ettringite formation and its thermal stability. *J. Thermal Anal. Calorim.* **65**, 655-660.

Zhou, Q. & Glasser, F.P. (2001): Thermal stability and decomposition mechanisms of ettringite at <120°C. *Cement and Concrete Research* **31**, 1333-1339.

*Received January 5, 2002, revised manuscript accepted July 22, 2002.*